

The Ventilated Pool: A Model of Subtropical Mode Water

W. K. DEWAR

The Florida State University, Tallahassee, Florida

R. M. SAMELSON

College of Oceanic and Atmospheric Sciences, Oregon State University, Corvallis, Oregon

G. K. VALLIS

Geophysical Fluid Dynamics Laboratory, Princeton University, Princeton, New Jersey

(Manuscript received 30 October 2003, in final form 14 July 2004)

ABSTRACT

An analytical model of subtropical mode water is presented, based on ventilated thermocline theory and on numerical solutions of a planetary geostrophic basin model. In ventilated thermocline theory, the western pool is a region bounded on the east by subsurface streamlines that outcrop at the western edge of the interior, and in which additional dynamical assumptions are necessary to complete the solution. Solutions for the western pool were originally obtained under the assumption that the potential vorticity of the subsurface layer was homogenized. In the present theory, it is instead assumed that all of the water in the pool region is ventilated and, therefore, that all the Sverdrup transport is carried in the uppermost, outcropping layer. The result is the formation of a deep, vertically homogeneous, fluid layer in the northwest corner of the subtropical gyre that extends from the surface to the base of the ventilated thermocline. This ventilated pool is an analog of the observed subtropical mode waters. The pool also has the interesting properties that it determines its own boundaries and affects the global potential vorticity–pressure relationship. When there are multiple outcropping layers, ventilated pool fluid is subducted to form a set of nested annuli in ventilated, subsurface layers, which are the deepest subducted layers in the ventilated thermocline.

1. Introduction

The structure of the subtropical thermocline has fascinated theorists and observationalists alike for many years for it is perhaps the single most prominent aspect of the ocean's stratification. Major features of that thermocline include broadly distributed pools of weakly stratified, low-potential-vorticity water, such as the "Eighteen-Degree Water" of the North Atlantic (Worthington 1959; McCartney 1982). These pools are known as "mode waters" because they appear as distinct modes in a census of water properties. The subtropical mode waters, observed in all subtropical ocean gyres, are of special interest for a variety of reasons, yet their origin remains relatively poorly understood.

Here, we propose a simple mechanism for the existence and maintenance of subtropical mode waters as a

large-scale dynamical component of the subtropical gyre circulation. A proximate mechanism for their formation, of course, is deep wintertime convection. However, this convection can only occur if the large-scale circulation maintains a weakly stratified volume of water with sufficiently small upper-ocean heat content. From this point of view, mode waters are part of the large-scale structure of the ocean thermocline, and must be understood within that context.

The model we propose here is, technically, a modest extension of the ventilated thermocline theory of the subtropical gyre developed by Luyten et al. (1983, hereinafter LPS). Although the ventilated thermocline is, as its name suggests, generally a stratified region, a striking feature of a number of numerical simulations of the subtropical thermocline that have reasonably small vertical diffusivity (Cox 1985; Samelson and Vallis 1997a, hereinafter SV97; Vallis 2000) is a thick recirculating thermostad extending down to the internal thermocline, particularly prominent in the northwest (or, more generally, pole-west corner) of the subtropical gyre, that resembles observed subtropical mode water.

Corresponding author address: R. M. Samelson, COAS, 104 Ocean Admin. Bldg., Oregon State University, Corvallis, OR 97331-5503.
E-mail: rsamelson@coas.oregonstate.edu

In this western region, ventilated thermocline theory suggests that a recirculating regime can form in which the circulation is controlled by some mechanism other than ventilation. One possibility, proposed by Luyton et al. (1983), is that this pool may be a region of homogenized potential vorticity. A separate, related, possibility involves the interaction of weak ventilation and homogenization. Such was examined in Dewar (1986), where it was argued that large-scale distributions of low potential vorticity waters naturally arose in these conditions. Convectively introduced mass anomalies in subsurface layers were balanced by eddy mass fluxes.

Although plausible, such mechanisms are based on the assumption of the downgradient diffusion of potential vorticity by eddies and, especially in regions like intense western boundary currents where mean advection may be important, this assertion cannot be justified. Note too that the original theory implicitly invokes eddy mechanisms in the pool region although they are required to be weak in order to fit within the homogenization formalism. The alternative hypothesis explored in the present study is that the western pool is wholly filled with ventilated fluid. That is to say, if there is no surface source for a given water mass, then we may suppose that no such water mass will exist. In the original theory, one must posit that the pool region is ventilated via eddy pathways for it is not ventilated by a steady inflow. Here we consider the possibility that those eddy fluxes are weak compared to the Ekman pumping mass flux. Thus, the present model casts the ventilated thermocline model into a self-consistent wholly noneddying form. If a nonventilated water mass is initially present, then we suppose that it slowly disappears from the pool region, expunged by the continuous downward Ekman pumping of surface water into the pool and a weak frictional flow down the pressure gradient. Our hypothesis is motivated by, and describes, the planetary geostrophic numerical model solutions computed by SV97, which contained an explicit western boundary layer, but no eddies and only minimal parameterized eddy fluxes.

In a two-layer model, this ventilated-pool hypothesis results in the mode-water region being represented by a single, thick upper layer, which forms above a second layer of zero thickness, and a third, quiescent layer or flat-bottom boundary beneath. As layers are added, the structure becomes more complicated and the ventilated pool may contain subducted layers, but the essential structure remains: a thick weakly stratified pool that forms the deepest part of the ventilated thermocline. An interesting complication is that the boundary of the pool region has vertical isopycnals (in the planetary geostrophic model) or layer interfaces and that these in general will be shocks, rather than passive features. That is, we may not necessarily suppose that the separate subregions making up the ventilated thermocline can be smoothly patched together or that a local solu-

tion exists to the equations of motion as needed that does not affect the solution in rest of the domain. However, by generalizing the model slightly and applying appropriate shock conditions, we show that solutions can be found that fit within the planetary geostrophic framework and that the consequence of the shock existence can be examined.

We show here that a model can be constructed that is based on the ventilated-pool hypothesis and satisfies the large-scale equations of motion. We examine the consequences of the mode water pool on the larger-scale circulation and compare qualitatively the quasi-analytical solutions so obtained with the numerical solutions of SV97. These solutions capture essential elements of the mode water found in that numerical model. We hope that the dynamical framework described here will also prove useful in the effort to understand mode waters and their role in the general circulation.

The model formulation and some specific solutions for the classical ventilated thermocline and the recirculating pool is the subject of section 2. The connection of these two zones is the subject of section 3, where the pool dynamics are considered in more detail and a generalization of the ventilated thermocline argument to properly allow for fronts is presented. A schematic extension to multiple outcrops with subduction of the model mode water is presented in section 4, which is followed by a concluding summary. Some technical computations are described in appendices.

2. A single-outcrop model

a. Formulation

We consider first a ventilated thermocline model (LPS) with two moving layers and a single outcrop, that being the simplest equation set that can illustrate the ideas. The thicknesses of layers 1 and 2 are denoted by h_1 and h_2 , respectively, and the corresponding layer interfaces are denoted by $z = -H_1$ and $z = -H_2$, respectively, where $H_1 = h_1$ and $H_2 = h_1 + h_2$. We will consider both the flat-bottom case of a two-layer ocean with $H_2 = \text{const}$ and the reduced-gravity case with two moving layers overlying a resting abyssal ocean and H_2 a function of position. The reduced gravity based on the density difference between layers j and $j + 1$ is denoted γ_j , where only γ_1 is considered for the flat-bottom case. Velocities and pressure are geostrophically related and layer pressures are connected to layer thicknesses via the usual formulas. A dynamically active variable in the lower layer of both models is the pressure, p_2 , which in the $2\frac{1}{2}$ -layer model is related to interface depth via $p_2 = \gamma_2 H_2$. The model is solved on a β plane, with Coriolis parameter $f = f_0 + \beta y$, where y is the meridional coordinate. The wind forcing, basin geometry, and nondimensionalization used in SV97 are employed here, so that the Ekman pumping is $w_E(x, y) = w_{E0} \cos 2\pi y$, $0 < y < 1$. At the eastern boundary $x = x_e$, $h_2 = H_2 = H_{2e} = \text{const}$, and $h_1 = 0$.

In the subtropical gyre ($0.25 < y < 0.75$), the solution has four distinct regimes (Fig. 1). For $y > y_2$, layer 2 is exposed to the surface forcing. There are three additional regimes in $y < y_2$, where layer 1 is exposed to the surface forcing: the central region, in which layer-2 fluid is ventilated, the shadow zone in the southeast, and the western pool region in the west. The bounding streamlines $x_s(y)$ and $x_p(y)$ separate the shadow zone and pool region, respectively, from the interior. Layer-2 fluid in the central, ventilated region is set in motion by the action of the wind in the outcrop zone $y > y_2$, but any layer-2 fluid in the shadow zone or pool region is isolated from direct contact with surface forcing.

b. The ventilated pool

Consider now the thermocline structure in the western pool region. For $y > y_2$, there is only one moving layer, and the geostrophic and Sverdrup balances may be solved in the usual way, giving

$$H_2 p_2 = \phi + H_2 p_{2e} \tag{2.1}$$

for the flat-bottom case and

$$\gamma_2 H_2^2 / 2 = \phi(x, y) + \gamma_2 \frac{H_{2e}^2}{2} \tag{2.2}$$

for the 2½-layer model, where $p_{2e} = p_2(x_e)$ and

$$\phi(x, y) = f^2 / \beta \int_{x_e}^x w_e dx. \tag{2.3}$$

South of the outcrop y_2 , the Sverdrup formulas generalize to

$$H_2 p_2 + \gamma_1 h_1^2 / 2 = \phi + H_2 p_{2e} \tag{2.4}$$

and

$$\gamma_1 h_1^2 / 2 + \gamma_2 H_2^2 / 2 = \phi + \gamma_2 \frac{H_{2e}^2}{2} \tag{2.5}$$

for the flat-bottom and reduced-gravity cases, respectively, as both layers are in motion. For $y < y_2$, the western limit of the ventilated interior is found by computing the trajectory of the characteristic $x_p(y)$ emanating from the point $x = x_w, y = y_2$, as described below (section 3a). For both the flat-bottom and reduced-gravity cases, these critical trajectories run through the interior, thus defining regions in layer 2 that are isolated from the outcrop and governed by processes other than ventilation (see, e.g., Figs. 1 and 2). LPS, for example, assume that the layer-2 potential vorticity is uni-

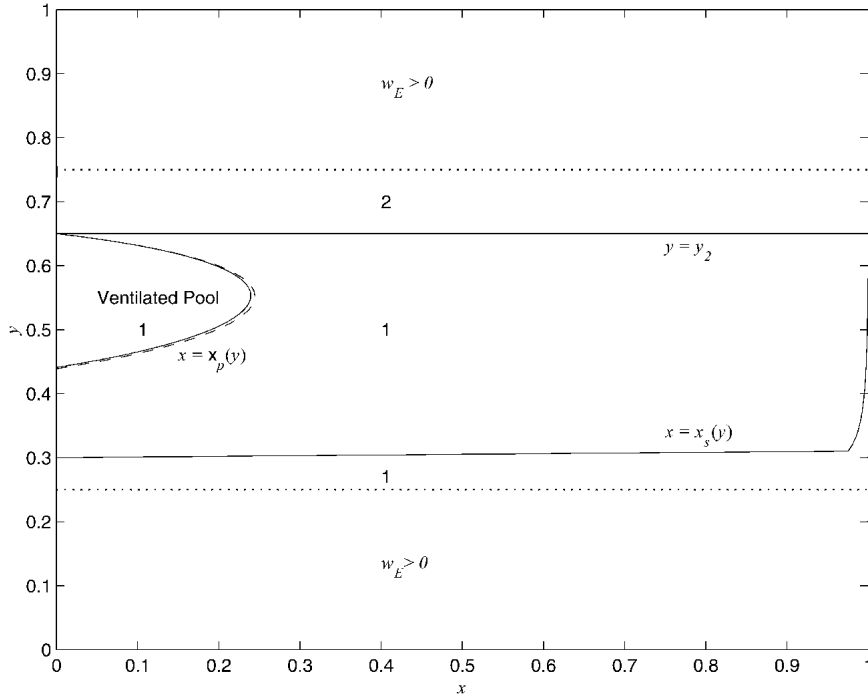


FIG. 1. Horizontal structure of the reduced-gravity model with the ventilated pool. The subtropical gyre is the region $0.25 < y < 0.75$, where $w_E < 0$. There is one subregion with layer 2 exposed to the surface forcing ($y > y_2 = 0.65$), and three with layer 1 exposed: the interior, in which the layer-2 fluid is ventilated, the shadow zone $x > x_s(y)$, and the ventilated-pool region $x < x_p(y)$. The number of the exposed layer in each of the four subregions is indicated. The western pool boundary characteristic (dashed) and the ventilated-pool shock trajectory (solid) are both shown. For this solution, $f_0 = 0.45$, $\beta = 1.1$, $\gamma_1 = 10$, $\gamma_2 = 50$, $H_{2e} = 0.1$, and $w_{E0} = 1$, with nondimensionalization as in SV97.

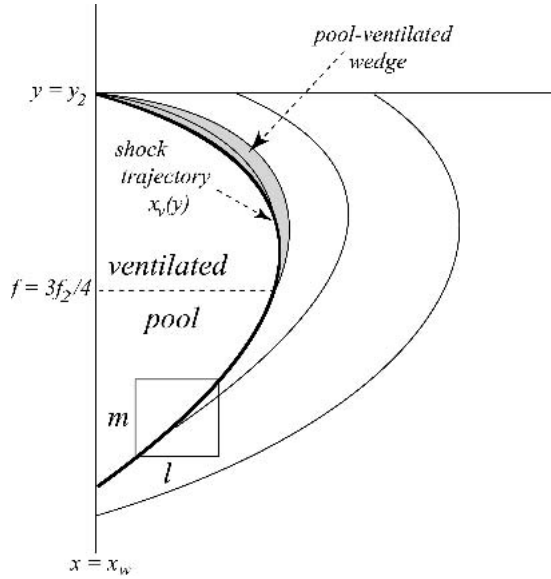


FIG. 2. Schematic of the front trajectory and characteristics. The box encloses an area encompassing the shock, and over which mass conservation is integrated in order to form the joining conditions. The quantities “ l ” and “ m ” denote the zonal and meridional lengths of the integration area, which in the limit converge in ratio to the slope of the front. Also shown are various characteristics determining the offshore front thickness. The shaded zone corresponds to the “pool ventilated” wedge emanating from the western edge of the outcrop; its width is exaggerated in the schematic. Control of h_+ passes to the regular ventilated thermocline at the latitude where $f = 3f_2/4$.

form in the pool region, and that the layer-2 thickness is continuous at the joint.

The central assumption of the present ventilated-pool theory is instead that layer-2 vanishes in the pool region:

$$h_2 = 0 \quad \text{and} \quad h_1 = H_1 = H_2, \quad \text{for } x < x_p(y). \quad (2.6)$$

Thus, in the pool region there is again only one moving layer; in the flat-bottom model, this layer fills the entire water column, while in the reduced-gravity model, the intermediate layer 2 vanishes, and the moving layer extends downward to the top of the stagnant layer 3. The Sverdrup solution in the ventilated-pool region is then

$$h_1 = \sqrt{\frac{2\phi + Hp_{2e}}{\gamma_1}} \quad (2.7)$$

for the flat-bottom model and

$$h_1 = \sqrt{\frac{2\phi + \gamma_2 H_{2e}^2}{\Gamma}} \quad (2.8)$$

for the reduced-gravity model, where $\Gamma = \gamma_1 + \gamma_2$ is the density difference between the moving layer (layer 1) and the quiescent fluid below (layer 3). The deep, homogeneous, recirculating surface layers (2.7) and (2.8) in the western subtropical gyre form the ventilated-pool mode-water analog in the single-outcrop flat-bottom

and reduced-gravity models, respectively. The thermocline depth h_1 in the ventilated-pool regions is thus determined by the Sverdrup relation, the eastern boundary depth of the deepest wind-driven layer, and the wind forcing.

A zonal cross section of the resulting solution of (2.8) in the middle of the subtropical gyre reveals the following structure (Fig. 3). The moving fluid farthest west consists entirely of upper-layer water and represents the “mode water” in this model. It is bounded on the east by the pool front. Just offshore of the front is a thin layer of pool-ventilated subsurface water. Farther offshore is the classical ventilated thermocline. The entire offshore zone is capped by a thin layer of warm water. A meridional cross section close to the western edge of the model domain will cut through the mode water, which will appear as a thick layer connected to the surface at the central latitudes of the gyre (Fig. 4). Despite the crude discretization of the vertical structure, these solutions may be usefully compared to the numerical model solutions of SV97. The analog of the ventilated pool in the numerical model is the weakly stratified region above the main thermocline on the western side of the basin (Fig. 5 and Fig. 6). The abrupt westward increases in the depths of isothermal surfaces above the main thermocline in the numerical model are analogs of the abrupt increase of layer-1 thickness across the pool boundary.

The assumption [(2.6)] that leads to the solutions (2.7) and (2.8) was originally motivated by the numerical model calculations analyzed by SV97. The essential factors that give rise to the formation of the vertically homogeneous, ventilated-pool structure in those numerical solutions can be readily identified. The key physical element is the lack of a source of layer-2 fluid in the pool region. The absence of such a source can be inferred from several properties of the SV97 model. The pool region is clearly isolated from the ventilated portion of layer 2 by the bounding streamline $x_p(y)$ or its analog in the SV97 solutions, and so there is no ventilation of layer 2 in the pool region. If the outcrop position were different, the structure of the pool would change accordingly but, by the very definition of the pool, there can be no ventilated source of layer-2 fluid in the pool. Similarly, surface cooling in the western boundary current cannot provide a source since the latitude at which layer-1 fluid is cooled to layer-2 temperatures in the boundary current defines the western limit of the outcrop and any such cooled surface fluid that returns to the subtropical gyre must enter the ventilated portion of layer 2 instead. The SV97 model is steady; therefore, there is no possible source from explicit eddy processes. Moreover, the SV97 western boundary current is essentially adiabatic (SV97; Samelson and Vallis 1997b; Samelson 1998), so parameterized eddy fluxes do not contribute significantly and consequently entrainment and mixing of layer-3 fluid also cannot provide a source. Examination of the spinup of the SV97

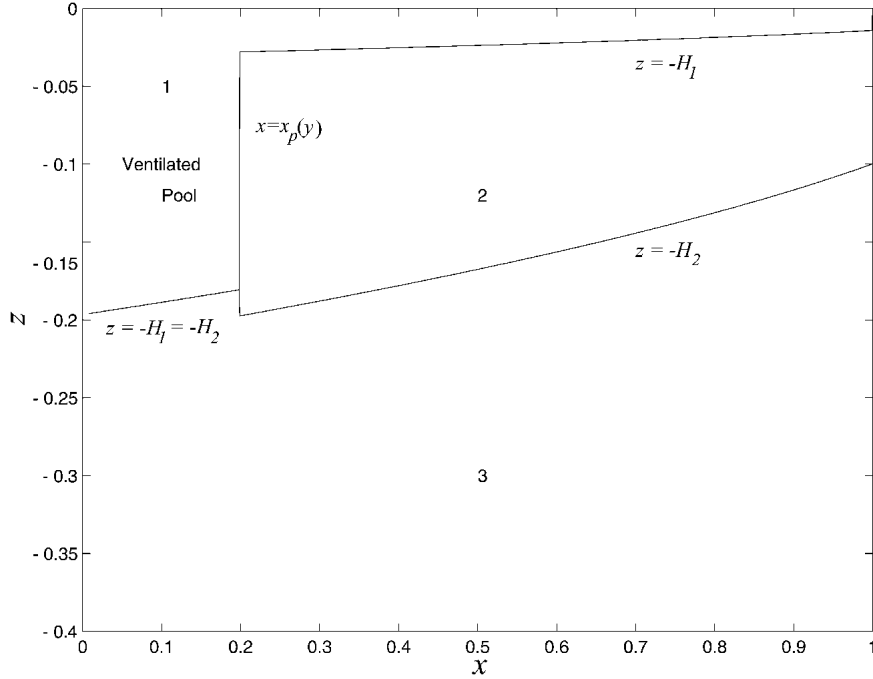


FIG. 3. Zonal cross section vs depth, at $y = 0.5$, of the reduced-gravity model with the ventilated pool. The layer numbers and interfaces are shown. The deep, homogeneous “subtropical mode water” layer in the ventilated pool region is located in the upper left, for $x < x_p(y)$. Layer 3 is quiescent and of arbitrary depth. Horizontal distance x and vertical distance z have been nondimensionalized by 5000 km and 5000 m, respectively. The constant depth of layer 2 at the eastern boundary $x = 1$ is $H_{2E} = 0.1$ (500 m).

solutions indicates that the exposed layer deepens in the west on the advective time scale until it reaches the depth of the main thermocline and carries all the Sverdrup transport, forming the homogeneous ventilated pool that we identify as an analog of subtropical mode water, while a classical ventilated regime develops to the east. Thus, these time-dependent solutions reach a stable steady ventilated-pool state without ever developing an analog of unventilated layer-2 fluid in the western-pool region.

In the ocean, of course, many processes may operate that are neglected in this analysis. However, motivated by the suggestive similarity between the model solutions and observed mode waters, we can rephrase the specific causes of the model pool structure as a hypothesis regarding the large-scale dynamical mechanisms that may support and maintain subtropical mode waters in the ocean:

- In the subtropical mode-water region, the dominant source of fluid in density classes above the main thermocline is downward surface Ekman pumping.
- Specifically, both adiabatic, lateral and diapycnal, turbulent eddy fluxes of fluid into density classes above the main thermocline in the subtropical mode-water region are small relative to surface Ekman pumping.

Some estimates of the relative importance of these processes in the ocean are discussed below in section 4.

3. Pool boundary dynamics

a. The western-pool boundary

In the standard ventilated thermocline theory, the western-pool boundary $x_p(y)$ in the flat-bottom or reduced-gravity model is determined as follows. The lower layer flow south of the outcrop line $y = y_2$ is governed in general by potential vorticity conservation, that is,

$$h_2/f = F_2(p_2). \quad (3.1)$$

From either (2.4) or (2.5), it is simple to show that any contour of constant potential vorticity (or, equivalently in the planetary geostrophic approximation, potential thickness h_2/f) is governed by

$$\phi_{fp_2} = \gamma_1 h_1 h_{1fp_2}, \quad (3.2)$$

where the notation “ $|_{p_2}$ ” denotes a derivative taken along a contour of constant p_2 . But because lines of constant p_2 correspond to constant h_2/f , the above becomes

$$\phi_{fp_2} = -\frac{\gamma_1 h_1 h_2}{f} = -\gamma_1 (H_2 - fF_{20})F_{20}, \quad (3.3)$$

where F_{20} denotes the constant value of potential thickness along the trajectory. This may be integrated to obtain an implicit expression for $x_p(y)$,

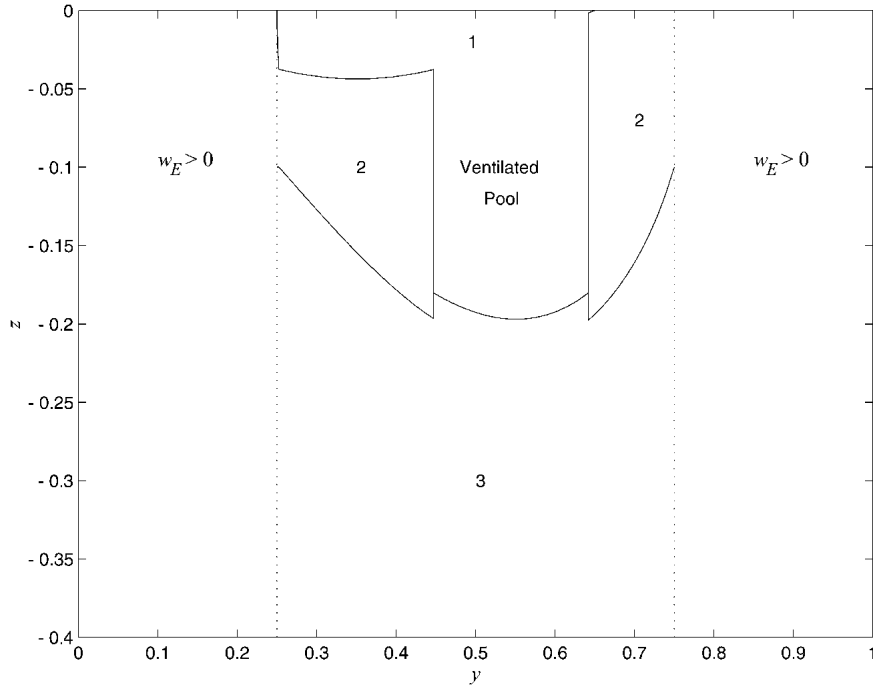


FIG. 4. Meridional cross section vs depth, at $x = 0.05$, of the reduced-gravity model with the ventilated pool. The layer numbers and interfaces are shown. The deep, homogeneous subtropical mode-water layer in the ventilated-pool region is located in the central portion of the section. Layer 3 is quiescent and of arbitrary depth. Horizontal distance x and vertical distance z have been nondimensionalized by 5000 km and 5000 m, respectively.

$$\phi[x_p(y), y] = \phi_w - \gamma_1 H F_{20} (f - f_2) + \gamma_1 \frac{F_{20}^2}{2} (f^2 - f_2^2), \quad (3.4)$$

where $H = H_2$ for the flat-bottom case and $H = H_{2w} = h_2(x_w, y_2)$ for the reduced-gravity case, and $\phi_w = \phi(x_w, y_2)$.

b. Flat-bottom case

The characteristic equation in (3.3) applies to both the flat-bottom and reduced-gravity models. It appears to be degenerate in the ventilated pool where, by assumption, $h_2 = 0$ and layer-2 characteristics cannot be defined. Nonetheless, it may be used to derive properties of the pool boundary, by considering arbitrarily small $h_2 > 0$, since this limit is well behaved: $\phi_f|_{p2} \rightarrow 0$ as $h_2 \rightarrow 0$. Thus, in the ventilated-pool theory, we may consider layer-2 characteristics in the recirculation pool in both cases to be governed by $\phi_f|_{p2} = 0$, so that the characteristics and Sverdrup contours coincide. Alternatively, the following argument can be rephrased in terms of layer-1 characteristics, but the present approach is simpler.

At the outcrop latitude f_2 , the characteristics in the ventilated zone, described by $h_1 = 0$, run parallel to those of the recirculating pool, described by $h_2 = 0$ [see (3.3)]. However, as the fluid moves south on the char-

acteristics, the recirculation zone continues to be described by $h_2 = 0$, while h_1 becomes positive in the ventilated zone. Thus by (3.3), the ventilated characteristics are governed by $\phi_f|_{p2} < 0$ while the pool characteristics continue to follow the Sverdrup contours (i.e., $\phi_f|_{p2} = 0$). The ventilated characteristics cross Sverdrup streamlines toward higher, and thus western, values as f decreases. This dual occupation of the same points in space by multiple characteristics is inconsistent with the straightforward application of the characteristics method. We conclude that globally smooth solutions of this hyperbolic boundary value problem are not possible and joining conditions must be considered. These conditions will yield new equations for the pool boundary $x_p(y)$. This boundary proves to consist, in general, of a shock trajectory $x_s(y)$ and a narrow adjacent “pool ventilated” region. For simplicity, we nonetheless denote the generalized ventilated-pool boundary by $x_p(y)$ in some parts of the discussion below.

Analytically joining the pool and the ventilated interior is rather complex, and it is useful first to examine the more accessible flat-bottom model. The condition governing discontinuities in this case is derived by integrating the potential vorticity conservation equation

$$J(p_2, h_2/f) = 0 \quad (3.5)$$

over an area covering the discontinuity. This area is defined by having two of its corners on the front tra-

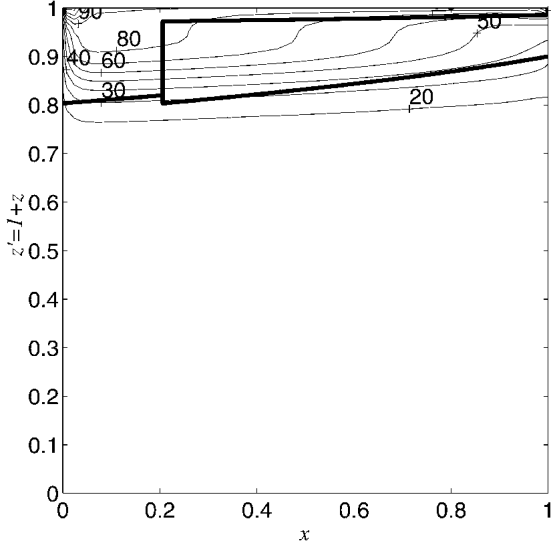


FIG. 5. Zonal cross section vs depth of the reduced-gravity model (thick solid lines) with the ventilated pool as in Fig. 3, overlaid on contours of temperature from a numerical solution of the continuously stratified planetary geostrophic model of SV97. The near-vertical isotherms above the main thermocline in the numerical solution are the analogs, on each isothermal surface, of the ventilated pool in the layer model. The planetary geostrophic model solution is influenced by friction, which reduces the zonal slope of the main thermocline, and thermal diffusion, both of which are neglected in the layer model.

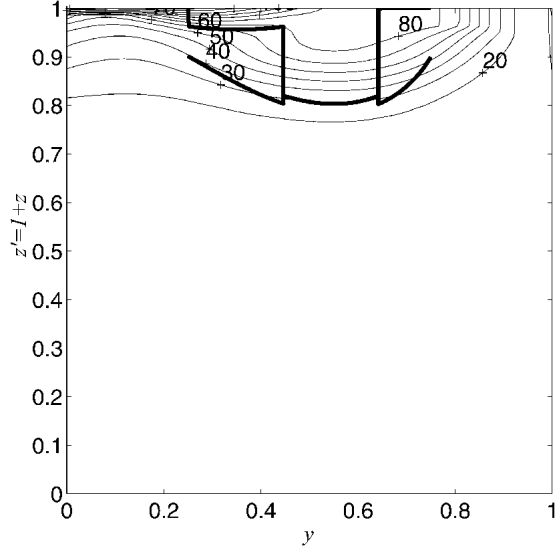


FIG. 6. Meridional cross section vs depth of the reduced-gravity model (thick solid lines) with the ventilated pool as in Fig. 4, overlaid on contours of temperature at $x = 0.1$ from a numerical solution of the continuously stratified planetary geostrophic model of SV97. The near-vertical isotherms above the main thermocline in the numerical solution are the analogs, on each isothermal surface, of the ventilated pool in the layer model. The planetary geostrophic model solution is influenced by friction, which reduces the zonal slope of the main thermocline, and thermal diffusion, both of which are neglected in the layer model.

jectory, but is otherwise rectangular (Fig. 2). The lengths of the two sides are given by m in the meridional direction and l in the zonal direction. The result of the area integration is

$$(\phi_y + \phi_x l/m) - \beta \gamma_1 / (f) \frac{[Hh_1^2/2 - h_1^3/3]}{[h_1]} = 0, \quad (3.6)$$

where the square brackets notation denotes the difference of the value of the enclosed quantity between the east and west sides of the domain. In the limit of vanishing l and m , their ratio converges to

$$\lim_{l,m \rightarrow 0} \left(\frac{l}{m} \right) \rightarrow \frac{\partial}{\partial y} x|_v, \quad (3.7)$$

the meridional slope of the front. A bit more algebra yields

$$\frac{d\phi_s}{df} = - \frac{\gamma_1 H}{f} \left[\frac{h_+ + h_-}{2} - \frac{h_+^2 + h_+ h_- + h_-^2}{3H} \right], \quad (3.8)$$

where h_+ (h_-) denotes the upper-layer thickness east (west) of the front and ϕ_s denotes the value of the barotropic streamfunction along the front. This is a differential equation governing the trajectory of the front through the general circulation.

For the front to exist, it is required that it be intersected on both sides by characteristics of the smooth solution (“smooth characteristics”). This is stated for the present problem as

$$\phi_f|_{h_-} \geq \phi_f|_v \geq \phi_f|_{h_+}, \quad (3.9)$$

where the first and third entries in the above denote trajectories of characteristics for the smooth part of the problem and the middle entry the trajectory of the shock. The above inequality reflects that, for decreasing f , the change in ϕ of the smooth characteristic governing h_- increase more slowly than either the same change for the shock or for the smooth characteristic governing h_+ . This way, the characteristics collide and are resolved by the presence of the shock. The equals signs in the above inequality correspond to limiting cases where the smooth solution characteristics are tangent to the shock. This recognition is key in the analysis to follow. What is to be avoided here, and what is not consistent with the concept of the shock, is for the smooth characteristics to radiate from the shock; for example, $\phi_f|_{h_+} < \phi_f|_v$. Now, given that the pool (with $h_1 = H$) always has characteristics that follow ϕ , it is sensible to pose $h_- = H$. Leaving h_+ unspecified for the moment, the shock equation in (3.8) becomes

$$\phi_f|_v = - \frac{\gamma_1}{f} \left(\frac{H^2}{6} + \frac{Hh_+}{6} - \frac{h_+^2}{3} \right), \quad (3.10)$$

and it is easy to show for all h_+ from 0 to H that the right-hand side is negative. The shock trajectory thus always climbs to larger ϕ for decreasing f , while the smooth characteristic for h_- always follows constant ϕ , rendering the postulate $h_- = H$ consistent. The value for h_+ is determined by the requirement that the smooth characteristic run parallel to the shock trajectory; that is,

$$\begin{aligned}\phi_{f|v} &= -\frac{\gamma_1 H}{f} \left(\frac{H}{6} + \frac{h_+}{6} - \frac{h_+^2}{3H} \right) \\ &= -\frac{\gamma_1}{f} h_+ (H - h_+) = \phi_{f|p_2},\end{aligned}\quad (3.11)$$

whose solution is $h_+ = H/4$. This implies the discontinuity in h_1 at (x_w, y_2) extends from $h_1 = H$ to $h_1 = H/4$. For smaller values of h_+ , the smooth characteristics do not press west fast enough to be swallowed into the shock.

The behavior of h_1 for $H/4 < h_1 < H$ is determined by the shock trajectory. It thus remains that h_1 for $0 < h_1 < H/4$ is part of a smooth thermocline for which the standard solution

$$\frac{h_2}{f} = \frac{H - h_1}{f} = G(p_2) \quad (3.12)$$

applies. The function G remains to be determined, however. The Sverdrup constraint (2.4) is everywhere valid, including through the front. The initial location of the front is (x_w, y_2) , so by (2.4),

$$Hp_2(h_1) = \phi_w - \frac{\gamma_1 h_1^2}{2} + Hp_{2e} \quad (3.13)$$

for the range $h_1 = 0 \rightarrow H/4$. Combining (3.12) and (3.13) then determines the function G :

$$G(p_2) = \frac{H - \sqrt{\frac{2H}{\gamma_1} (p_{2e} + \phi_w/H - p_2)}}{f_2} = \frac{H - h_1}{f}. \quad (3.14)$$

Equation (3.14), when combined with (2.4), determines both p_2 and h_1 on all characteristics that can be traced back to (x_w, y_2) . This part of the thermocline may be referred to as ‘‘pool ventilated,’’ as it has a potential vorticity that is set by the pool condition $h_1 = H$.

As the shock is followed south from y_2 , its eastern face starts to entrain pool-ventilated water. In fact, it turns out that $h_+ = H/4$ during this phase of front evolution because parts of the smooth thermocline thicker than this run into the shock, while those thinner move away from it. Further, the pool-ventilated characteristic emanating from $h_1 = 0$ and the ventilated thermocline characteristic emanating from $h_1 = 0$ remain parallel always, as they both start from the same location and

have the same characteristic equation [(3.3)]. Thus, at the latitude where $f = 3f_2/4$, $h_{2+}/f = H/f_2$, signaling a switch from pool-ventilated water to normal ventilated water on the offshore front edge (see Fig. 2).

c. Reduced-gravity case

The flat-bottom model illustrates the essential features of the pool boundary calculation, but does so in the unrealistic environment of a rigid lower boundary. The reduced-gravity setting is in this sense a much more natural model of the real ocean, but is algebraically much more tedious. Nonetheless, an analysis like that outlined above applies to the reduced-gravity model, as shown below.

The first hurdle is to develop a shock trajectory equation like (3.8). The procedure is again to consider an integral of the layer-2 potential vorticity equation over a small region around the shock (Fig. 2), although the calculations are more involved. The details are given in appendix A and only the results are quoted here.

Define

$$\begin{aligned}F(h_2) &= \frac{\gamma_1 \gamma_2 h_2^2}{2\Gamma} - \frac{\phi \gamma_2}{\sqrt{\gamma_1 \gamma_2}} \left[\sin^{-1} \left(\sqrt{\frac{\gamma_1 \gamma_2}{2\phi \Gamma}} h_2 \right) \right. \\ &\quad \left. - \sqrt{\frac{\gamma_1 \gamma_2}{2\phi \Gamma}} h_2 \sqrt{1 - \frac{\gamma_1 \gamma_2}{2\phi \Gamma} h_2^2} \right].\end{aligned}\quad (3.15)$$

The shock equation is

$$\phi_{f|w} = \frac{-\frac{1}{f} F(h_2)}{\left(\frac{\sqrt{\gamma_1 \gamma_2}}{\gamma_1} \sin^{-1} \left[\sqrt{\frac{\gamma_2 \gamma_1}{2\phi \Gamma}} h_2 \right] \right)} \quad (3.16)$$

for the 2½-layer problem, where it has been assumed that $h_{2-} = 0$.

Recall that $h_1 = 0$ along $f = f_2$ until $x = x_w$, at which point $h_2 = 0$. Simple algebra shows that at the discontinuity, $h_1 = \sqrt{(2\phi_w + \gamma_2 H_{2e}^2)/\Gamma}$. Thus h_1 changes in the front from this value to a minimum of 0, while h_2 changes from 0 to $h_2 = \sqrt{(2\phi_w + \gamma_2 H_{2w}^2)/\gamma_2} = h_{2w}$. Following the flat-bottom analysis, the layer-2 thickness for which the characteristics along the shock parallel the smooth thermocline thickness must be computed. This is obtained by equating (3.3) with (3.16). Although it may be consistently assumed that $h_{2-} = 0$, it is still necessary to solve the resulting equation for the initial h_{2+} numerically. This value will be referred to as h_{2c} . Then, for all h_2 from h_{2c} to h_{2w} , the smooth functional relationship linking the potential thickness and pressures must be determined. To do so uses the special form of the Sverdrup potential at ϕ_w

$$\gamma_1 \frac{h_1^2}{2} + \frac{\gamma_2 H_2^2}{2} = \phi_w + \frac{\gamma_2 H_{2e}^2}{2}. \quad (3.17)$$

The relation between h_2 and H_2 for general ϕ is

$$H_2 = \frac{\gamma_1 h_2}{\Gamma} + \frac{\sqrt{2\phi\Gamma + \Gamma\gamma_2 H_{2e}^2 - \gamma_1 \gamma_2 h_2^2}}{\Gamma}, \quad (3.18)$$

which can be used to diagnose the functional relationship between p_2 and h_1 . Combining with the Sverdrup relation yields

$$h_1 = \frac{(\gamma_1 f_2 - \Gamma f) h_2}{\Gamma f} + \frac{\sqrt{2\phi_w \Gamma + \gamma_2 H_{2e}^2 \Gamma - \gamma_1 \gamma_2 f_2^2 h_2^2 / f^2}}{\Gamma}, \quad (3.19)$$

which governs the connection between h_1 and h_2 on any characteristic that can be traced to (x_{2w}, y_2) . This function and the Sverdrup relation give h_2 in the pool-ventilated zone. Again, the ventilated thermocline characteristic starting from (x_w, f_2) with $h_1 = 0$ must be parallel to the pool-ventilated characteristic with $h_1 = 0$. So, the value of p_2 hitting the shock on the east should be monitored and, when it exceeds p_{2w} emanating from (x_w, f_2) , h_{2+} must be computed from the standard ventilated thermocline theory. In either case, values for both h_{2-} and h_{2+} can be determined for any interior oceanic point, and the front equation in (3.16) can be integrated in latitude to yield a new value for $\phi|_v$.

The frontal pool boundary computed in this way lies to the west of the original western-pool boundary, which forms the eastern limit of the pool-ventilated wedge; on the eastern side of the original pool boundary, the circulation is governed by standard ventilated thermocline theory (Fig. 1).

4. Discussion

a. Subduction

In the simple models discussed above, the entire meridional variation of surface density in the subtropical gyre is concentrated at the zonal outcrop of layer 2, and the ventilated pool region in the northwest corner of the gyre is completely filled by a single, deep, homogeneous layer of fluid extending from the surface outcrop to the base of the main thermocline. It is straightforward to generalize this conceptual model to the case in which the meridional variation of density in the subtropical gyre is distributed across several layer outcrops, as in the original LPS ventilated thermocline theory. The main complication is that there are a number of distinct regions to consider, each requiring a separate calculation to determine the various layer depths.

Consider a standard three-layer reduced-gravity model with two layer outcrops, each at a constant latitude. The moving layers are labeled 1, 2, 3 from the top as usual, with corresponding densities ρ_1 , ρ_2 , and ρ_3 , the outcrop between layer 1 and layer 2 being at latitude y_2 ,

and that between layers 2 and 3 at y_3 (Fig. 7). The standard multiple-outcrop ventilated thermocline is complicated by the splitting of western-pool and shadow-zone boundary trajectories at each outcrop in the various layers. In the present situation, the complexity is increased by the need to solve the shock equations. For the present illustrative purposes, we dispense with these complexities by fixing the pool boundaries at the original western-pool boundary locations that would obtain for corresponding single-outcrop models, and neglecting the shadow zone entirely. This is adequate to provide a semiquantitative schematic solution of the two-outcrop model. The explicit formulas are given in appendix B.

The main result of the two-outcrop model is that the ventilated pool that forms from the northern outcrop will be subducted at the southern outcrop, forming a thick, homogenous subsurface layer. The details of this structure depend on the latitude of the southern outcrop. A western-pool region arises at a given outcrop if the flow at the western edge of the outcrop is eastward that is, if the outcrop is north of the latitude of maximum Ekman pumping. If the southern outcrop in the two-outcrop model is south of this latitude, the characteristics of layer 2 will be directed westward and no ventilated pool will form in layer 1 (Fig. 7). In this case, the subducted ventilated pool and the shallow layer-1 cap above it will extend to the western boundary (Fig. 8). These solutions develop a shallow ventilated thermocline structure above the subducted pool that closely resembles the SV97 solutions (Fig. 6).

If both outcrops are north of the latitude of maximum Ekman pumping, however, there will be two pool

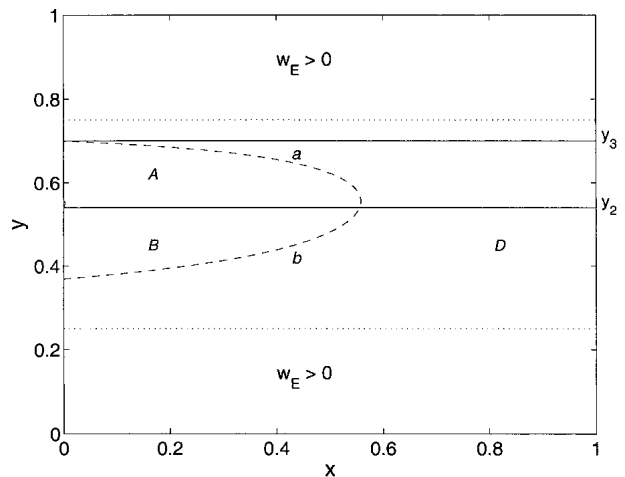


FIG. 7. Horizontal structure of the three-layer, two-outcrop model with ventilated pool in layer 2 only. The outcrop latitude of layer 2 is $y_2 = 0.54$, just equatorward of the latitude of maximum Ekman pumping, so the characteristics in the subsurface layer 2 are all directed westward, and no ventilated pool forms in layer 1, while the layer-2 ventilated pool is subducted at $y = y_2$. For this solution, $\gamma_2 = 20$, $\gamma_3 = 30$, and $y_3 = 0.7$, and the other parameters are as in Fig. 1.

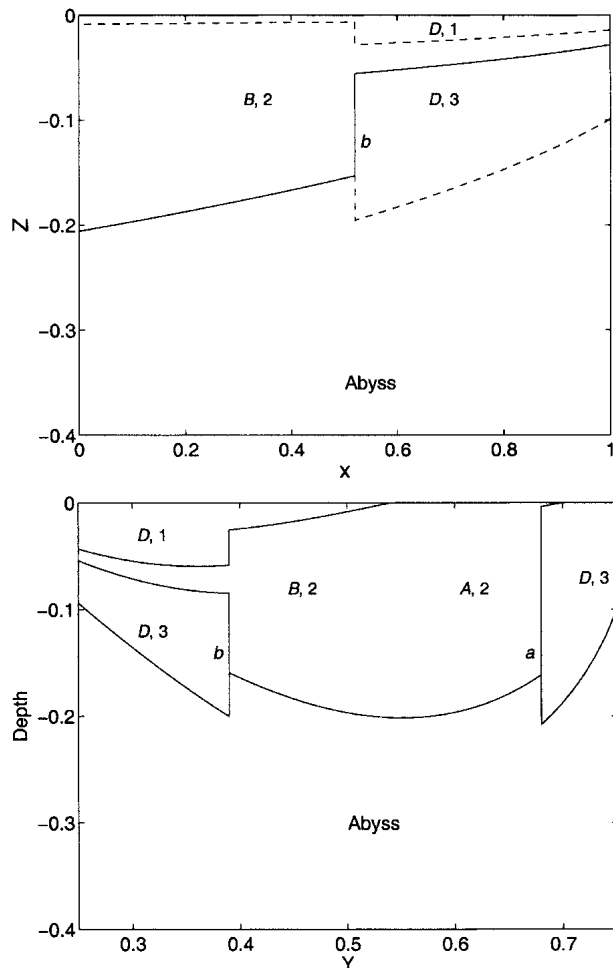


FIG. 8. (top) Zonal cross section at $y = 0.5$ and (bottom) meridional cross section at $x = 0.1$, corresponding to the solution of Fig. 7. The uppercase and lowercase letters correspond to the regions and boundaries in Fig. 7, respectively, and the numbers indicate the fluid layer. The stagnant layer 4 is labeled "Abyss" and the shadow zone is omitted. The upper interface in the meridional cross section is analogous to the shallow ventilated thermocline in the SV97 solutions (Fig. 6).

boundaries, one emanating from the western edge of each of the two outcrops (Fig. 9). In this case, the southern outcrop ($y = y_2$) will cross the northern, outer pool boundary, dividing the latter into two segments. Denote these segments a and b (Fig. 9). Denote the region west of the northern segment (a) and north of $y = y_2$ by A , and the region west of the southern segment (b) and east of the southern, inner pool boundary (c) by B . Also, denote the region west of the inner pool boundary c by C , and the regions east of the outer pool boundary (a and b) by D . In regions A and B , then, there are no characteristics of layer 3 that thread back to the surface and therefore within A and B there is no layer-3 water. Furthermore, on region C there are no characteristics of layer-2 water that thread back to the surface and therefore within C all of the water is layer-1

water. Zonal sections through regions C , B , and D will show three distinct thermocline structures, from west to east: an inner ventilated pool, with a single thick layer of moving layer-1 fluid in region C ; an intermediate regime with moving fluid in the shallow, exposed layer 1 and the thick, subducted ventilated-pool layer-2 annulus in region B ; and the standard eastern ventilated thermocline regime in region D (Fig. 10).

This results of this simplified three-layer reduced-gravity calculation may be compared with the SV97 numerical solutions, in which the mode-water analog appears as a continuous, nested set of annuli on successive isopycnal surfaces (Fig. 5 and Fig. 6). In zonal cross-section, these appear as short, near-vertical segments above the main thermocline on the $T = 50, 60, 70,$ and 80 isotherms (Fig. 5). This structure is the natural extension to continuous stratification of the two-outcrop conceptual picture described above: each vertical isopycnal segment, lying between the shallow, ventilated part of the surface to the east and the deep, unventilated part of the surface to the west, is an analog in the continuous model of the single subducted annulus that lies between the two pool boundaries in the two-outcrop model (Fig. 10). The capped ventilated-pool structure that arises when the southern outcrop is south of the latitude of maximum wind stress curl (Fig. 8) is apparent in cross sections of the SV97 numerical solutions (Fig. 6).

The three-layer model is sufficient to illustrate the subduction of the ventilated pool and the associated formation of the nested annulus and shallow ventilated thermocline structures. Introducing additional layers and outcrops would lead to a set of several nested an-

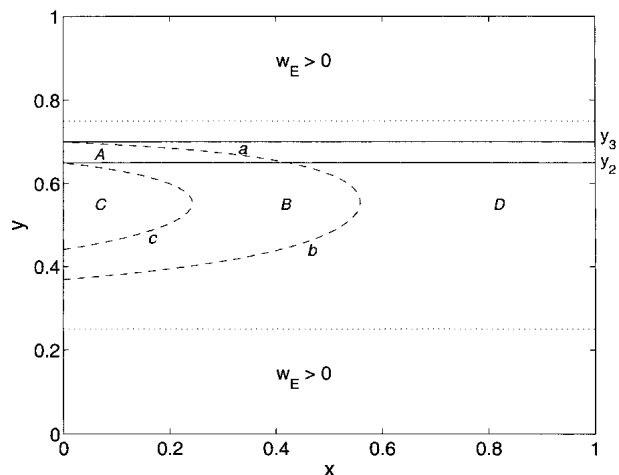


FIG. 9. Horizontal structure of the three-layer, two-outcrop model as in Fig. 7 but for $y_2 = 0.65$, with ventilated-pool regions in layers 1 and 2. The outer pool boundary, marked a and b , corresponds to the boundary of characteristics in layer 3 that do not trace back to the surface, and the boundary marked c corresponds to similar characteristics of layer 2. The regions A , B , and C are ventilated-pool regimes, while region D is the classical ventilated-thermocline regime.

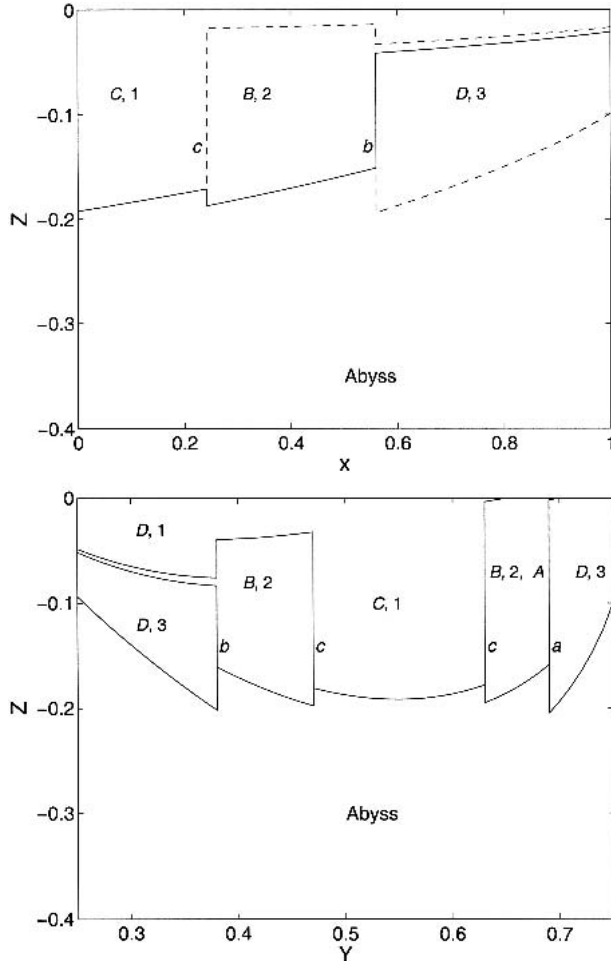


FIG. 10. (top) Zonal cross section at $y = 0.55$ and (bottom) meridional cross section at $x = 0.1$, corresponding the solution of Fig. 9. The uppercase and lowercase letters correspond to the regions and boundaries in Fig. 9, respectively, and the numbers indicate the fluid layer. The stagnant layer 4 is labeled “Abyss” and the shadow zone is omitted. The subducted annulus labeled “B, 2” in the zonal cross section is analogous to the vertical segments of isothermal surfaces above the main thermocline in the SV97 solutions (Fig. 5).

nuli and shallow ventilated layers, resulting in a structure similar to the isothermal surfaces in the SV97 numerical solutions (e.g., Fig. 5 and Fig. 6). As in the two-outcrop model, the total lateral density gradient across the ventilated pool will be determined by the surface boundary conditions and the geometry of the outcrops. However, even in the continuously stratified SV97 solutions, the transition in depth on each isopycnal occurs abruptly (Fig. 5), as a front, in agreement with the present model, and this in turn suggests that such fronts will tend to obtain an inherent dynamical character of their own. The horizontal gradients in the mode-water analog from the SV97 solutions are less apparent in meridional sections (Fig. 6). Note that, despite having lateral density gradients, the fluid in the

continuously stratified ventilated pool is nearly homogeneous vertically and so will have low potential vorticity throughout.

The SV97 solutions used a planetary geostrophic numerical model. Similar ventilated-pool mode-water features appear generically in primitive equation model simulations of subtropical gyre circulation (e.g., Cox 1985). These can often be identified by the tongues of low potential vorticity immediately above the main thermocline (e.g., Cox 1985; Fig. 5) associated with the weakly stratified, subducted annuli.

b. Jets and eddies

In the layer model, the lateral density gradients in the ventilated pool and at its boundary are represented by vertical interfaces between the adjacent layers. Associated with these fronts in the layer model will be intense baroclinic jets with infinitesimal thickness. In the continuous limit (SV97), these jets will spread out laterally over the width of the pool and the corresponding baroclinic shears will be weakened, as they evidently are in the planetary geostrophic numerical solution. Nonetheless, such areas are almost undoubtedly prone to baroclinic instability (Samelson 1999), and so may provide an important source of eddy energy in these regions; indeed, Henning and Vallis (2004) observe that the mode-water region is a region of strong mesoscale activity. The corresponding eddy fluxes could act to reduce the lateral density gradients within the pool that are associated with the nested annuli structure discussed above.

It is possible to make rough estimates of the size of the associated fluxes, which are generally relevant to the neglect of eddy processes in the theory, as well as to the specific case of the unstable baroclinic jets. These estimates may be compared to the downward Ekman flux into the ventilated pool, which provides the only source of ventilated-pool fluid in the present model. The average downward Ekman velocity $\overline{w_{ek}}$ for this area is a little weaker than the typical values quoted for subtropical gyres because the formation zone for the mode waters is close to the zero Ekman pumping line. Thus, $\overline{w_{ek}} \approx -0.8 \times 10^{-6} \text{ m s}^{-1}$. The amplitude of the lateral eddy-driven mass flux, $w_{eddy} \approx KV^2h$, can be crudely estimated as an effective velocity w_{eddy} by assuming a lateral diffusion coefficient of $1000 \text{ m}^2 \text{ s}^{-1}$ acting on a 300-m-deep layer extending laterally a radius of 500–2500 km. The resulting values are $w_{eddy} \approx 1.2 - 0.05 (\times 10^{-6} \text{ m s}^{-1})$, and so can be comparable to $\overline{w_{ek}}$. Diapycnal velocities w_d can also be estimated based on an interior diffusivity of $10^{-5} \text{ m}^2 \text{ s}^{-1}$ operating on a 300-m-thick water mass and are quite small at $w_d \approx 3 \times 10^{-8} \text{ m s}^{-1}$. From these estimates, it is well established that diabatic fluxes are relatively weak. The neglect of eddy fluxes is not as clearly supported, and these may be expected to modify the present large-scale dynamical results.

A related feature of note is the abrupt change, at the

bounding streamline $x_p(y)$, of the depth of the main thermocline. This discontinuity arises from the difference between the reduced gravities across the main thermocline in the ventilated pool region (Γ) and in the adjacent ventilated interior (γ_2). As $x_p(y)$ is approached from the ventilated interior, the depth of the main thermocline approaches the value

$$H_{2p}^+ = \left[\frac{2\phi(x_p, y_2) + \gamma_2 H_{2e}^2}{\gamma_2} \right]^{1/2}, \quad (4.1)$$

while from the ventilated pool, it approaches

$$H_{2p}^- = \left[\frac{2\phi(x_p, y_2) + \gamma_2 H_{2e}^2}{\Gamma} \right]^{1/2}. \quad (4.2)$$

Clearly, these two thicknesses cannot be equal. The effect of the westward-increasing density difference across the main thermocline across the pool boundary (or across the pool itself, in the continuous limit) is to decrease the depth of the main thermocline toward the west relative to the depth it would obtain if the warm fluid were confined near the surface. The geostrophic shears associated with these changes in the depth of the main thermocline may also be baroclinically unstable. It is conceivable that the convergent eddy-driven heat fluxes observed by Henning and Vallis (2004) at the base of the main thermocline in eddy-permitting primitive equation simulations are related to this baroclinic energy source.

c. Air–sea heat fluxes

The model of the existence and maintenance of subtropical mode waters that we propose here does not explicitly address the role of air–sea heat exchange in mode-water formation. In fact, with a boundary current that arranges to return the subducted fluid adiabatically to the subtropical gyre at the same latitudes where it was previously exposed to the surface, our model mode water could be seen—except for a volume flux equal to the net downward Ekman pumping over the pool area, which must then escape to the subpolar gyre—as an essentially adiabatic, steady, recirculating pool. In contrast, many studies of subtropical mode water have focused on wintertime formation of homogeneous columns of fluid by convective overturning that is induced by air–sea heat exchange and on the relation between mode water and the intense heat loss from the ocean to the atmosphere in the western boundary currents and their extensions that lie on the rim of the mode-water regions. From the point of view of the present model, however, the seasonal air–sea exchanges would represent a literally superficial mechanism with little dynamical influence on the large-scale circulation processes that support the existence and maintenance of the mode water pool. Similarly, we cannot exclude the possibility that eddy processes may be important components of the dynamics of observed ocean mode water,

but it should be clear that they play no explicit or implicit role in the present model.

5. Summary

A simple modification to standard ventilated thermocline theory yields an appealing model of the large-scale dynamical mechanisms that support and maintain subtropical mode water as an essential component of the subtropical gyre circulation. The modification consists in assuming that there are no significant sources of unventilated, recirculating fluid and, consequently, that the western pool region is entirely filled with ventilated fluid. The resulting ventilated pool is a vertically homogeneous layer of fluid in the northwest corner of the subtropical gyre, which extends from the surface to the main thermocline and carries the entire Sverdrup transport in this region. This ventilated pool is a natural model of subtropical mode water. With multiple outcropping density layers, or continuous stratification, the mode-water pool comprises a set of nested annuli of successively subducted, vertically homogeneous fluid layers. Lateral gradients in the pool are controlled by large-scale surface conditions and geometry. In this model, the subtropical mode water is ventilated, in the sense of LPS. It is the deepest such ventilated layer, and so forms the base of the ventilated thermocline and the wind-driven motion in the northwest portion of the subtropical gyre.

Future work might usefully address the dynamic and thermodynamic mechanisms by which the recirculating subsurface layer of fluid interacts with the western boundary current and the atmosphere, and explicitly consider the time scales on which this occurs. The structure of mode water suggested by the model will be particularly prone to baroclinic instability, which can be expected to modify the circulation. We hope that this model will provide a useful point of reference for understanding mode water in more complete numerical models and that these ideas will be useful in the analysis of such models and in further attempts to understand the important role of mode waters in ocean and global climate dynamics.

Acknowledgments. This research was supported by the National Science Foundation (NSF), Grants OCE-0220700 and OCE-0220884 (WKD), OCE-9907854 and OCE-0218812 (RMS), and OCE-0412345 (GKV).

APPENDIX A

A Front Trajectory Equation for a Reduced-Gravity Model

The equation governing the trajectory of a front through the general circulation can be obtained by integrating

$$J(p_2, h_2/f) = 0 \quad (\text{A.1})$$

over a small region enclosing the shock (Fig. 2). The result corresponds to the conservation of layer-2 mass through the shock and may be written

$$M_N - M_S + M_E - M_W = 0, \quad (\text{A.2})$$

where $M_{N,S,E,W}$ denotes the mass flux through the north ($y = y_N$), south ($y = y_S$), east ($x = x_E$), and west ($x = x_W$) sides of the domain, respectively. For the remainder of this appendix, M_W will be ignored, as h_2 is assumed to vanish in the ventilated pool; M_N is by design determined solely by northward velocity, thus

$$M_N = \int_{x_W}^{x_E} (h_2 p_{2x} / f_N) dx = \frac{1}{f_N} \int_{p_{2W}}^{p_{2E}} h_2 dp_2, \quad (\text{A.3})$$

where the subscripts “W” and “E” denote values west and east of the front respectively, and $f_N = f(y_N)$. Layer-2 pressure and thickness are related via

$$p_2 = \frac{\gamma_2 \gamma_1 h_2}{\Gamma} + \frac{\gamma_2 \sqrt{2\Gamma\phi - \gamma_2 \gamma_1 h_2^2}}{\Gamma} \quad (\text{A.4})$$

through the front by the Sverdrup constraint. Thus (A.3) yields three integrals:

$$M_N = \left[\frac{\gamma_1 \gamma_2 h_2^2}{\Gamma} \right]_{h_{2-}}^{h_{2+}} + \frac{\gamma_2}{2f_N \Gamma} \int_{\phi_W}^{\phi_E} \frac{2\Gamma h_2 d\phi}{\sqrt{2\Gamma\phi - \gamma_1 \gamma_2 h_2^2}} - \frac{\gamma_2^2 \gamma_1}{\Gamma f_N} \int_{h_1}^{h_2} \frac{h_2^2 dh_2}{\sqrt{2\Gamma\phi - \gamma_1 \gamma_2 h_2^2}}. \quad (\text{A.5})$$

It is useful to distinguish in the above equation between “fast” variables like h_2 , which on a zonal section through the front change rapidly, and “slow” variables like ϕ , which are insensitive to the presence of the front. This permits the second integral to be ignored relative to the first and third because, as $x_E \rightarrow x_W$, the second integral is proportional to $\phi_E - \phi_W \rightarrow 0$. In contrast, the other integrals involve $O(1)$ changes in the fast variables. The third item in (A.5) is however rendered easily integrable if the slowness of ϕ is exploited to replace it by the constant value $\phi[(x_E + x_W)/2, y_N]$. In summary, defining

$$F(h_2) = \frac{\gamma_1 \gamma_2 h_2^2}{2\Gamma} - \frac{\phi \gamma_2}{\sqrt{\gamma_1 \gamma_2}} \left(\sin^{-1} \left[\sqrt{\frac{\gamma_1 \gamma_2}{2\phi \Gamma}} h_2 \right] - \sqrt{\frac{\gamma_1 \gamma_2}{2\phi \Gamma}} h_2 \sqrt{1 - \frac{\gamma_1 \gamma_2}{2\phi \Gamma} h_2^2} \right) \quad \text{and} \quad (\text{A.6})$$

$$M_N = \frac{F(h_{2+})}{f_N} - \frac{F(h_{2-})}{f_N} = \frac{F(h_{2+})}{f_N}, \quad (\text{A.7})$$

the latter equality being due to $h_{2-} = 0$. A similar formula can be written for M_S . Note that the result of the integration is a formula that depends only on the

end point thickness, h_{2+} . This is a slow variable east of the front, so the difference $M_N - M_S$ can be written as

$$M_N - M_S = M_y \delta_y, \quad (\text{A.8})$$

where $\delta_y = y_N - y_S$.

The eastern face mass flux, M_E can be written as

$$M_E = \int \mathbf{u}_2 h_2 \cdot \mathbf{n}_E dl, \quad (\text{A.9})$$

where \mathbf{n}_E is the eastward-pointing unit vector normal to the front

$$\mathbf{n}_E = \frac{\mathbf{i} - x_{y|v} \mathbf{j}}{\sqrt{1 + (x_{y|v})^2}}.$$

The quantity $x_{y|v}$ denotes the meridional derivative of the shock trajectory $x(y)$ and the line integration traces the front slightly to its east. A little algebra then shows

$$M_E = - \int \frac{p_{2y|v} h_2 dy}{f}. \quad (\text{A.10})$$

Using (A.4) in the above returns three integrals, all of which contribute at first order in δy . Computing $\partial M / \partial y$ and gathering the results in (A.2) yields (3.16).

APPENDIX B

The Three-Layer Model

We give here explicit expressions for the three-layer model solutions described in section 4a. Let the reduced gravities be defined by

$$\gamma_{13} = g \frac{\rho_3 - \rho_1}{\rho_0} = \gamma_1 + \gamma_2, \quad \gamma_{14} = \gamma_1 + \gamma_2 + \gamma_3,$$

and

$$\gamma_{24} = \gamma_2 + \gamma_3. \quad (\text{B.1})$$

The layer thickness are denoted h_1 , h_2 , and h_3 and the coordinates of the interfaces are denoted η_1 , η_2 , and η_3 such that $\eta_1 = -h_1$, $\eta_2 = -(h_1 + h_2)$, and $\eta_3 = -(h_1 + h_2 + h_3)$. Also, $f_i = f(y_i)$, x_e is the longitude of the eastern boundary of the domain, h_{3e} is the thickness of layer 3 at the eastern boundary, and $W(y)$ is the value of the wind stress curl.

The solution is then calculated as follows (see Fig. 9).

- 1) Within region *A* all of the moving fluid is layer 2 fluid, and beneath this is abyssal fluid of density ρ_4 . Thus, the layer depth is calculated as in a one-layer ventilated thermocline model, and as in the pool region of the one-layer model, but with an appropriate value for the reduced gravity determined by the density contrast between layer 2 and layer 4.
- 2) At y_1 layer 2 is subducted under layer 1, and so within region *B*, the pool region consists of layer-1 and layer-2 fluid. Layer 2 conserves its potential vor-

ticity, and this is given by its value at y_2 . Effectively, then, the layer depths are calculated as in a two-layer ventilated thermocline model, with moving layers of density ρ_1 and ρ_2 , along with the abyss ρ_4 .

- 3) In region C all of the moving fluid is layer-1 fluid, and beneath this is abyssal fluid. Thus, the calculation proceeds as in item 1 above except with a different value of the reduced gravity (and of course a different wind field, appropriate to the different latitude).
- 4) Outside of the pool regions, the layer depths are calculated in the standard way for a three-layer model. There will in general be the usual shadow zone in the eastern part of the domain, necessary to satisfy the no-normal flow condition at the eastern boundary, and the usual need to specify the (constant) depth of layer 3, H_3 , at the eastern boundary. Note that the layer depths will in general be discontinuous at the pool boundaries, as in the single-outcrop model.

The layer thicknesses are given by region C :

$$\begin{aligned} \eta_1 &= -h_1 = -\sqrt{D_1^2 + \frac{\gamma_3 h_{3e}^2}{\gamma_{14}}}, \\ \eta_2 &= \eta_1, \eta_3 = \eta_1 \quad (h_2 = h_3 = 0), \end{aligned} \quad (\text{B.2})$$

where the Sverdrup depth D_1 is given by

$$D_1 = \frac{2f^2}{\beta\gamma_{14}}(x - x_e)W(y); \quad (\text{B.3})$$

region B :

$$\begin{aligned} \eta_2 &= -\sqrt{D_2^2 + \frac{(\gamma_3 h_{3e}^2 / \gamma_{24})}{1 + (\gamma_1 / \gamma_{24})(1 - ff_2)^2}}, \\ \eta_1 &= (1 - ff_2)\eta_2, \eta_3 = \eta_2, \end{aligned} \quad (\text{B.4})$$

where

$$D_2 = \frac{2f^2}{\beta\gamma_{24}}(x - x_e)W(y); \quad (\text{B.5})$$

region A :

$$\eta_2 = -\sqrt{D_2^2 + (\gamma_3 h_{3e}^2 / \gamma_{24})}, \eta_1 = 0, \eta_3 = \eta_2. \quad (\text{B.6})$$

Outside of these regions, that is in region D , the layer depths are given by the standard formulas for a three-layer ventilated thermocline model.

The various layer depths of the regions for the case shown in Fig. 7 are calculated in a similar fashion, although there is now no region C .

REFERENCES

- Cox, M. D., 1985: An eddy resolving numerical model of the ventilated thermocline. *J. Phys. Oceanogr.*, **15**, 1312–1324.
- Dewar, W. K., 1986: On the potential vorticity structure of weakly ventilated isopycnals: A theory of subtropical mode water maintenance. *J. Phys. Oceanogr.*, **16**, 1204–1216.
- Henning, C. C., and G. K. Vallis, 2004: The effects of mesoscale eddies on the main subtropical thermocline. *J. Phys. Oceanogr.*, **34**, 2428–2443.
- Luyten, J. R., J. Pedlosky, and H. Stommel, 1983: The ventilated thermocline. *J. Phys. Oceanogr.*, **13**, 292–309.
- McCartney, M., 1982: The subtropical recirculation of mode waters. *J. Mar. Res.*, **40** (Suppl.), 427–464.
- Samelson, R. M., 1998: Large-scale circulation with locally enhanced vertical mixing. *J. Phys. Oceanogr.*, **28**, 712–726.
- , 1999: Note on a baroclinic analogue of vorticity defects in shear. *J. Fluid Mech.*, **382**, 367–373.
- , and G. K. Vallis, 1997a: Large-scale circulation with small diapycnal diffusion: The two-thermocline limit. *J. Mar. Res.*, **55**, 223–275.
- , and —, 1997b: A simple friction and diffusion scheme for planetary geostrophic basin models. *J. Phys. Oceanogr.*, **27**, 186–194.
- Vallis, G. K., 2000: Large-scale circulation and production of stratification: Effects of wind, geometry and diffusion. *J. Phys. Oceanogr.*, **30**, 933–954.
- Worthington, L. V., 1959: The 18° Water in the Sargasso Sea. *Deep-Sea Res.*, **5**, 297–305.